JOURNAL OF VIROLOGY, Sept. 1999, p. 7853–7859 Vol. 73, No. 9
0022-538X/99/$04.00+0

Induction of Apoptosis in Murine Coronavirus-Infected Cultured Cells and Demonstration of E Protein as an Apoptosis Inducer

SUNGWHAN AN,[1]† CHUN-JEN CHEN,[1,2] XIN YU,[3]‡ JULIAN L. LEIBOWITZ,[3] AND SHINJI MAKINO[1,2]*

Department of Microbiology and Institute for Cellular and Molecular Biology, The University of Texas at Austin, Austin, Texas 78712[1]; Department of Microbiology and Immunology, The University of Texas Medical Branch at Galveston, Galveston, Texas 77555-1019[2]; and Department of Pathology and Laboratory Medicine, Texas A&M University Health Science Center, College Station, Texas 77843-1114[3]

Received 10 February 1999/Accepted 26 May 1999

We demonstrated that infection of 17Cl-1 cells with the murine coronavirus mouse hepatitis virus (MHV) induced caspase-dependent apoptosis. MHV-infected DBT cells did not show apoptotic changes, indicating that apoptosis was not a universal mechanism of cell death in MHV-infected cells. Expression of MHV structural proteins by recombinant vaccinia viruses showed that expression of MHV E protein induced apoptosis in DBT cells, whereas expression of other MHV structural proteins, including S protein, M protein, N protein, and hemagglutinin-esterase protein, failed to induce apoptosis. MHV E protein-mediated apoptosis was suppressed by a high level of Bcl-2 oncogene expression. Our data showed that MHV E protein is a multifunctional protein; in addition to its known function in coronavirus envelope formation, it also induces apoptosis.

Apoptosis (or programmed cell death) is an important process in the development and homeostasis of multicellular organisms (18, 28, 43). In most cases, apoptosis is executed by activating a proteolytic system involving a family of proteases called caspases. Caspases participate in a cascade that is triggered in response to proapoptotic signals and culminates in cleavage of a set of proteins, resulting in cell death (12, 45). Apoptosis also represents a highly efficient defense mechanism against virus infection; apoptosis aids in removal of viral proteins and nucleic acids by the infected host. Two types of apoptotic stimuli eventually lead to apoptosis of virus-infected cells. Virus-infected cells undergo apoptosis by the attack of cytotoxic cells, including cytotoxic T cells and natural killer cells (50, 51, 62). Virus-infected cells may also undergo a cell-autonomous apoptosis without the attack by immune cells; accumulated data show that many viruses induce apoptosis in infected cells (25, 29, 37, 38, 42, 44, 47, 48, 56, 59). In addition, different viruses have developed a variety of strategies to interfere with host cell apoptosis (1, 9–11, 16, 23, 24, 39, 41, 58, 65). Inhibition of apoptosis often enhances replication and accumulation of these viruses.

Coronaviruses are enveloped RNA viruses that cause gastrointestinal and upper respiratory tract illnesses in animals and humans. These range in severity from a very serious neonatal enteritis in domestic animals to the common cold in humans. Although coronavirus infections are usually acute, some coronaviruses cause persistent neurotropic infections in animals (2, 49, 61). Among the coronaviruses, mouse hepatitis virus (MHV) is one of the best characterized in terms of its pathogenesis and molecular biology. MHV causes various diseases, including hepatitis, enteritis, and encephalitis, in rodents (13, 61). In addition, infection with certain strains of MHV causes demyelination in rodents, and MHV-induced demyelination has been used as an excellent model system for human demyelinating diseases, such as multiple sclerosis (2, 27, 34, 61).

MHV contains a 32-kb-long positive-sense, single-stranded RNA genome (32, 35, 46) that encodes 11 open reading frames which are expressed through the production of genome-size mRNA and six to eight species of subgenomic mRNAs (33, 36). These mRNAs form a 3′ coterminal nested-set structure, and generally, each MHV-specific protein is translated from each subgenomic mRNA. Two viral envelope proteins, the 23-kDa M protein and the 9.6-kDa E protein, play an important role in the formation of MHV envelope (5, 30, 60). The E protein is present in only minute amounts in coronavirus particles (64). Expression of the coronavirus M and E proteins is sufficient for the production of virus-like particles (3, 5, 60). In addition to the M and E proteins, the coronavirus envelope includes the 180/90-kDa S protein, which binds to coronavirus receptor (17) and forms the characteristic coronavirus peplomer. Some coronaviruses contain a 65-kDa hemagglutinin-esterase (HE) protein, which is not essential for coronavirus replication in cell cultures, although it may affect viral pathogenicity (63). The coronavirus genomic RNA is associated with a 50- to 60-kDa N protein forming a helical nucleocapsid (55).

Infection of coronaviruses in cultured cells usually results in the death of infected cells. Eleouet et al. (19) demonstrated that infection of coronavirus transmissible gastroenteritis virus (TGEV) induces caspase-dependent apoptosis in several cell lines. Their data suggest that TGEV infection may lead to apoptosis via cellular oxidative stress. Belyavskyi et al. (4) showed that MHV strain 3 (MHV-3) infection of cultured macrophages induces apoptosis, while it is not clear whether MHV-3-induced apoptosis is caspase dependent. It is not known whether any TGEV- or MHV-3-specific proteins are responsible for the induction of apoptosis.

In the present study we first investigated whether MHV infection induced apoptosis in established cell lines. We examined morphological changes which occurred during MHV infection of 17Cl-1 cells (obtained from Susan Baker, Loyola University Chicago). Cells were cultured in a medium con-

* Corresponding author. Mailing address: Department of Microbiology and Immunology, The University of Texas Medical Branch at Galveston, Galveston, TX 77555-1019. Phone: (409) 772-2323. Fax: (409) 772-5065. E-mail: shmakino@utmb.edu.

† Present address: Department of Microbiology and Immunology, Stanford University, Stanford, CA 94305.

‡ Present address: Department of Biology, California Institute of Technology, Pasadena, CA 91125.

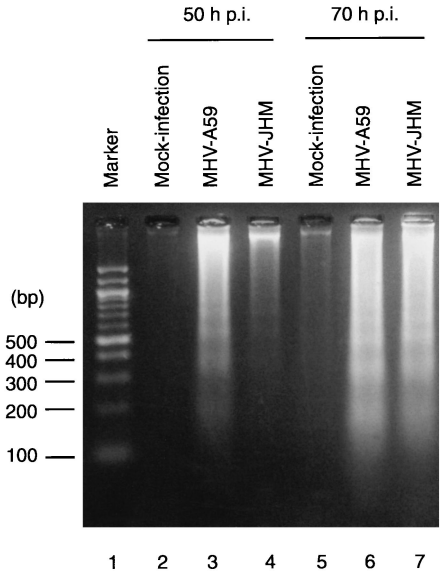

FIG. 1. DNA fragmentation analysis of 17Cl-1 cells infected with MHV. Low-molecular-weight DNA was isolated at 50 and 70 h p.i. from MHV-A59-infected, MHV-JHM-infected, or mock-infected cells, as indicated. Samples were electrophoresed in a 2% agarose gel and visualized with ethidium bromide.

sisted of Dulbecco's modified minimum essential medium (DMEM) containing sodium pyruvate (JRH Biosciences), heat-inactivated 10% fetal calf serum, and 0.1 mg of kanamycin per ml. Shrinkage, rounding, and aggregation were the cytopathic effect (CPE) observed in 17Cl-1 cells that were infected with the A59 strain of MHV (MHV-A59) at a multiplicity of infection (MOI) of 5. The CPE was evident at 20 h postinfection (p.i.), and the extent of CPE became stronger until about 70 h p.i., the last time point of our observation. Many of the cells showing CPE became detached from the plates; in MHV-A59-infected cells, about 90, 70, and 50% of cells were attached to the plates at 36, 50, and 70 h p.i., respectively. CPE appeared more quickly in cells infected with MHV-A59 than in cells infected with the JHM strain of MHV (MHV-JHM), whereas after about 50 h p.i., the extents of CPE in the two infected cultures were similar.

We examined MHV-infected 17Cl-1 cells for the presence of internucleosomal DNA cleavage, an event commonly observed in apoptotic cells. At various times after infection, cells attached to the plates were scraped by using a rubber policeman and combined with those floating in the medium. Low-molecular-weight apoptotic DNA fragments were collected as described by Hinshaw et al. (25) and then separated by agarose gel electrophoresis (Fig. 1). A sign of internucleosomal DNA cleavage, which appeared as a low level of smearing of DNA in agarose gel electrophoresis, was first detected at 36 h p.i.; a DNA ladder was not evident at this time (data not shown). At 50 h p.i., a DNA ladder was evident both in MHV-A59-infected cells and MHV-JHM-infected cells, and the extent of DNA fragmentation increased at 70 h p.i. (Fig. 1). The DNA cleavage appeared more slowly in MHV-JHM-infected cells (Fig. 1, lane 4) than in MHV-A59-infected cells, while at 70 h p.i., the extents of DNA fragmentation in MHV-JHM-infected cells and in MHV-A59-infected cells were similar. A DNA ladder was not detected in the mock-infected cells at 50 or 70 h p.i. (Fig. 1). These data demonstrated that extensive internucleosomal DNA cleavage occurred late in infection in MHV-infected 17Cl-1 cells. We used the terminal deoxynucleotidyltransferase-mediated dUTP nick end labeling (TUNEL) assay (ApoAlert DNA fragmentation assay kit; Clontech) to further confirm DNA fragmentation in MHV-A59-infected 17Cl-1 cells (Fig. 2). DNA fragmentation was found in the MHV-infected 17Cl-1 cells that remained attached to the plate at 36 and 48 h p.i. Approximately one-quarter of the infected cells were TUNEL positive. Almost no TUNEL-positive cells were observed in the mock-infected cultures. Characterization of DNA fragmentation by agarose gel electrophoresis and TUNEL assay unambiguously demonstrated internucleosomal DNA cleavage in MHV-infected 17Cl-1 cells.

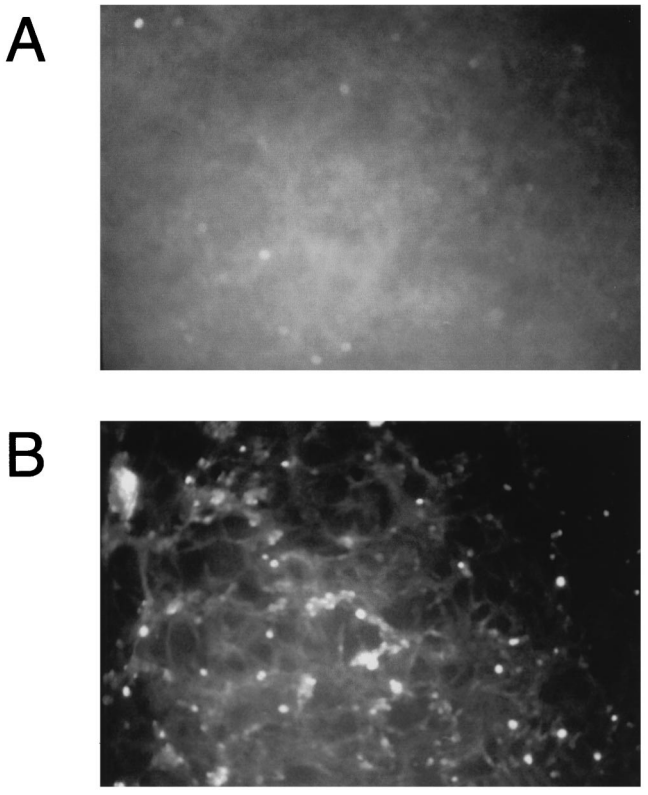

FIG. 2. DNA fragmentation in MHV-infected 17Cl-1 cells. 17Cl-1 cells were mock infected (A) or infected with MHV-A59 at an MOI of 5 (B). At 36 h p.i., cells attached to the plates were examined by TUNEL assay for DNA fragmentation.

To confirm that MHV-infected 17Cl-1 cells were undergoing apoptosis, MHV-A59-infected 17Cl-1 cells were stained with the fluorescent dye Hoechst 33342. Cells at 80% confluence were mock infected or infected with virus. At various times p.i., cells were collected, washed with phosphate-buffered saline (PBS), and resuspended in 100 μl of PBS. Cells were fixed by first slowly adding 200 μl of fixing solution (3:1 methanol:acetic acid) and then adding additional fixing solution up to 2 ml. The samples were then incubated at room temperature for at least 1 h. After centrifugation at 1,000 rpm for 10 min, cells were resuspended in 400 μl of fixing solution. Approximately 100-μl volumes of cell suspensions were deposited on microscopic slides and air dried. Cells were stained with a drop of staining solution (50% glycerol, 50% 0.1 M Tris-HCl [pH 7.4], 1 μg of Hoechst 33342 per ml), coverslipped, and observed under a fluorescence microscope. In the mock-infected culture, the majority of cells contained intact nuclei at 68 h p.i. In MHV-infected 17Cl-1 cultures examined at 68 h p.i., cells which had detached from the culture dish showed chromatin condensa-

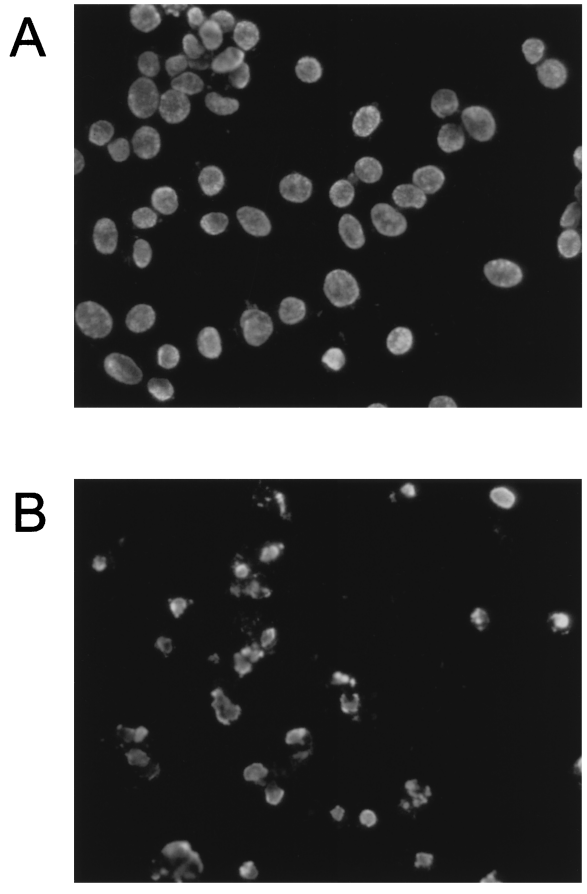

FIG. 3. Chromatin condensation in 17Cl-1 cells infected with MHV. 17Cl-1 cells were mock infected (A) or infected with MHV-A59 at an MOI of 5 (B). At 68 h p.i., mock-infected cells (A) and floating cells in MHV-infected culture media (B) were collected and stained with Hoechst 33342.

tion (Fig. 3). Hoechst staining of cells which remained attached to the plate at 68 h p.i., demonstrated that MHV-infected cells showing CPE also underwent chromatin condensation (data not shown). These data demonstrated that apoptosis was induced in MHV-infected 17Cl-1 cells, and the strong apoptotic signs were evident late in infection.

To test whether binding of MHV to MHV receptors or some unidentified substances, other than MHV, present in the inoculum induced apoptosis, the MHV-A59 preparation that was used in the above experiments was inactivated by irradiation of inoculum with UV light prior to addition to 17Cl-1 cells. The infectivity of UV-irradiated samples was less than 1 PFU. After incubation for 1 h at 37°C, the inoculum was removed and the cells were incubated for up to 46 h. Neither CPE nor internucleosomal DNA cleavage was observed in the cells that underwent this treatment (data not shown), demonstrating that binding of MHV to MHV receptors alone or unidentified substances, which may be present in the inoculum, did not induce apoptosis. Replication of MHV was necessary for inducing apoptosis.

In the very late stage of this study, we noticed that changing cell culture condition significantly affected CPE phenotype and induction of apoptosis. When MHV-A59-infected 17Cl-1 cells were incubated in a medium containing DMEM from a different vender (GIBCO-BRL), fusion-type CPE was detected at 10 h p.i., and DNA ladder was clearly detected as early as 24 h p.i. (data not shown). There were several differences in the contents of two batches of DMEM used in this study; one major difference was that DMEM from GIBCO-BRL lacked sodium pyruvate, while DMEM used in most of our other experiments contained sodium pyruvate. Our present data and previous findings of apoptosis in TGEV-infected cultured cells (19) and in MHV-3-infected cultured macrophages (4) established that apoptosis is one mechanism of cell death in coronavirus-infected cells.

We examined whether apoptosis was induced in another MHV-susceptible cell line, DBT (26). DBT cells show extensive cell fusion after overnight infection with MHV-A59, and the fused cells detach from the plates. Floating fused cells and the small number of cells that were still attached to the plates were collected at 12, 36, and 48 h p.i. Gel electrophoresis of low-molecular-weight DNA fragments from these samples and TUNEL assay at 12 h p.i. showed no sign of DNA fragmentation (data not shown), demonstrating that MHV infection in these cells did not induce internucleosomal DNA cleavage. Few signs of apoptosis (demonstrated by Hoechst staining) and very limited cell fusion were observed in DBT cells that were infected with MHV-A59 at a low cell density (data not shown), indicating that prevention of cell fusion did not induce apoptosis. These studies demonstrated that apoptosis was not a universal event among MHV-infected established cell lines. DBT cells are derived from an astrocytoma isolated from CDF1 mice (26), while 17Cl-1 cells are a line of spontaneously transformed mouse BALB/c 3T3 cells (54); DBT cells and 17Cl-1 cells were derived from different organs of different strains of mice. The difference in the apoptotic response to MHV infection between DBT cells and 17Cl-1 cells may be determined by the difference in the origin of organs and/or difference in the strain of mice. In the case of MHV-3-induced apoptosis in macrophages, differences in the genetic background play a role for the severity of apoptosis (4).

To determine whether MHV-induced apoptosis was caspase dependent, we studied the effect of Z-Asp-Glu-Val-Asp-FMK (Z-DEVD-fmk), an irreversible and cell-permeable inhibitor of caspase-3, on the induction of apoptosis in MHV-A59-infected 17Cl-1 cells. When caspase-3 is activated by apoptotic stimuli, it activates a caspase-activated DNase (CAD), which is present in the cytosol complexed with its inhibitor ICAD. Caspase-3 cleaves ICAD and allows CAD to translocate to the nucleus and degrade DNA (20). 17Cl-1 cells were incubated for 2 h with 40 or 80 μM Z-DEVD-fmk (Enzyme Systems Products, Livermore, Calif.) prior to MHV-A59 infection. After MHV infection at an MOI of 1 for 1 h at 37°C, cells were incubated in the presence of 40 or 80 μM Z-DEVD-fmk for 24 h. At 24 h p.i., the Z-DEVD-fmk was replenished, and the cultures were incubated for an additional 24 h. At 48 h p.i., low-molecular-weight DNAs were extracted. Agarose gel electrophoresis of apoptotic DNA fragments showed that addition of 80 μM Z-DEVD-fmk in the medium strongly inhibited internucleosomal DNA cleavage (Fig. 4). Apoptosis was only modestly inhibited at a concentration of 40 μM Z-DEVD-fmk. These data showed that caspase-3 inhibitor Z-DEVD-fmk suppressed the MHV-induced apoptosis, demonstrating that MHV-induced apoptosis in 17Cl-1 cells was caspase dependent. A comparison of one-step growth curves of MHV in 17Cl-1 cells in the presence and absence of 80 μM Z-DEVD-fmk indicated that suppression of caspase-3 activity did not affect MHV growth (data not shown). Our present data and the previous finding that TGEV-induced apoptosis is inhibited by the pancaspase inhibitor Z-VAD.fmk (19) indicate that coronavirus infection induces caspase-dependent apoptosis (12, 45).

To examine whether expression of any individual MHV

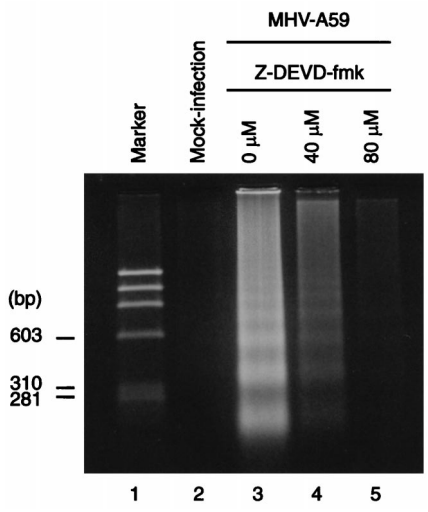

FIG. 4. Effect of Z-DEVD-fmk on MHV-induced apoptosis. 17Cl-1 cells were mock infected or incubated with medium containing Z-DEVD-fmk (dissolved in dimethyl sulfoxide) at a concentration of 0 (dimethyl sulfoxide only), 40, or 80 μM, as indicated, before and after infection with MHV-A59. At 48 h p.i., low-molecular-weight DNA was extracted and separated in a 2% agarose gel.

structural protein could induce apoptosis, cells were infected with a series of recombinant vaccinia viruses, each of which expresses a single MHV structural protein, and tested for internucleosomal DNA cleavage and chromatin condensation. We used the IHD strain of vaccinia virus (VV-IHD) as our wild-type (wt) virus and a series of recombinant vaccinia viruses expressing MHV-JHM M protein (vJM) (52), MHV-JHM N protein (vJN) (53), and MHV-JHM HE protein (vJHE) (52) and that expressing S protein of the cl-2 variant of MHV-JHM [RVV t(+)] (57). To generate recombinant vaccinia virus expressing MHV-JHM E protein (VV-E), a DNA fragment containing the coding sequence of the MHV-JHM E protein was amplified by PCR. In the PCR, the nucleotides at −3 (G) and +4 (T) were changed to an A and a G, respectively, in an attempt to increase the translation efficiency of RNA transcripts from the E protein gene (31). The PCR product was cloned into the vaccinia virus transfer vector pSC11ss. The E gene was subsequently put under the control of a strong synthetic vaccinia virus late promoter (14) by transferring the entire coding sequence of the MHV-JHM E gene to the pMJ601 vector. Recombinant vaccinia viruses were isolated by established procedures (8, 40). Internucleosomal DNA cleavage occurred in wt VV-IHD-infected 17Cl-1 cells (data not shown) and not in VV-IHD-infected DBT cells (Fig. 5), suggesting that VV-IHD infection induced apoptosis in 17Cl-1 cells but not in DBT cells. These data implied that 17Cl-1 cells were not suitable for subsequent studies. Accordingly, we used DBT cells for further studies. DBT cells were independently infected with VV-IHD, VV-E, vJM, RVV t(+), vJN, or vJHE, at an MOI of 1. Low-molecular-weight DNA was extracted from total cell populations at various times p.i. Extensive DNA fragmentation occurred in VV-E-infected cells (Fig. 5) but not in cells that were infected with VV-IHD or other recombinant vaccinia viruses (data not shown). Accumulation of E protein in VV-E-infected cells was evident at 30 h p.i. by radioimmunoprecipitation of [^{35}S]methionine-labeled E protein by anti-E protein antibody (data not shown). The amount of MHV N protein, M protein, HE protein, and S protein present in cells infected with recombinant vaccinia viruses was significantly higher than the amount of E protein contained in VV-E-infected cells (data not shown). Thus, the absence of DNA fragmentation in the other recombinant vaccinia virus-infected cells was not due to a low expression level of the MHV N, M, HE, and S proteins. Hoechst staining of vaccinia virus-infected cells at 42 h p.i. showed chromatin condensation in VV-E infected cells but not in wt VV-IHD-infected cells (Fig. 6). These data demonstrated that MHV E protein expression induced apoptosis in DBT cells. This is the first demonstration that one of the coronavirus proteins can induce apoptosis. MHV E protein is an acylated low-molecular-weight integral membrane protein, which is synthesized in small amounts in MHV-infected cells (64). E protein is membrane associated and is transported to the cell surface in coronavirus-infected cells (64). E protein is important for coronavirus assembly, particularly for the formation of the virus envelope (3, 5, 30, 60). As the MHV E protein also induced apoptosis, it is a multifunctional protein.

Overexpression of the Bcl-2 oncoprotein delays or blocks apoptosis induced by various stimuli, including virus infection (21, 25, 37). To determine if high-level Bcl-2 expression blocked MHV E protein-induced apoptosis, we established a DBT cell line stably expressing the *bcl-2* gene. To establish stable transformants, DBT cells at approximately 60% confluence were transfected with plasmid pZIPbcl-2, which expresses the human *bcl-2* gene (37), or its parental plasmid, pZIPneo (7), which lacks the *bcl-2* gene. Both plasmids contain a neomycin resistance gene (37). Lipofection reagent (GIBCO-BRL) was used for transfection. A pool of DBT cells that were stably transfected with pZIPbcl-2 (DBT/bcl-2) or with pZIPneo (DBT/neo) was selected by adding 800 μg of Geneticin (GIBCO-BRL) per ml to the culture medium. Expression of Bcl-2 was examined by an immunoblot assay. Cell lysates from DBT, DBT/neo, or DBT/bcl-2 cell cultures were submitted to sodium dodecyl sulfate-polyacrylamide gel electrophoresis, and separated proteins were transferred to Trans-Blot transfer polyvinylidene difluoride membranes (Bio-Rad). The membranes were probed with a mouse anti-human Bcl-2 monoclonal antibody (Boehringer Mannheim) at a dilution of 1:100 in PBS, followed by a 1:1,000 dilution of a sheep anti-mouse immunoglobulin G secondary antibody conjugated to

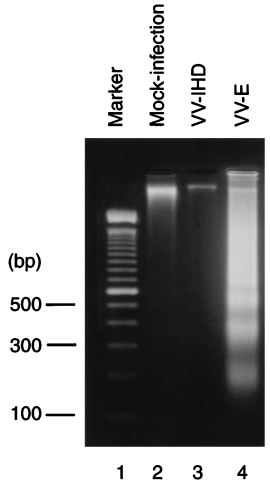

FIG. 5. Induction of apoptosis in VV-E-infected DBT cells. DBT cells were mock infected or infected with VV-IHD or VV-E at an MOI of 1, as indicated. At 45 h p.i., low-molecular-weight DNA was extracted and separated in a 2% agarose gel.

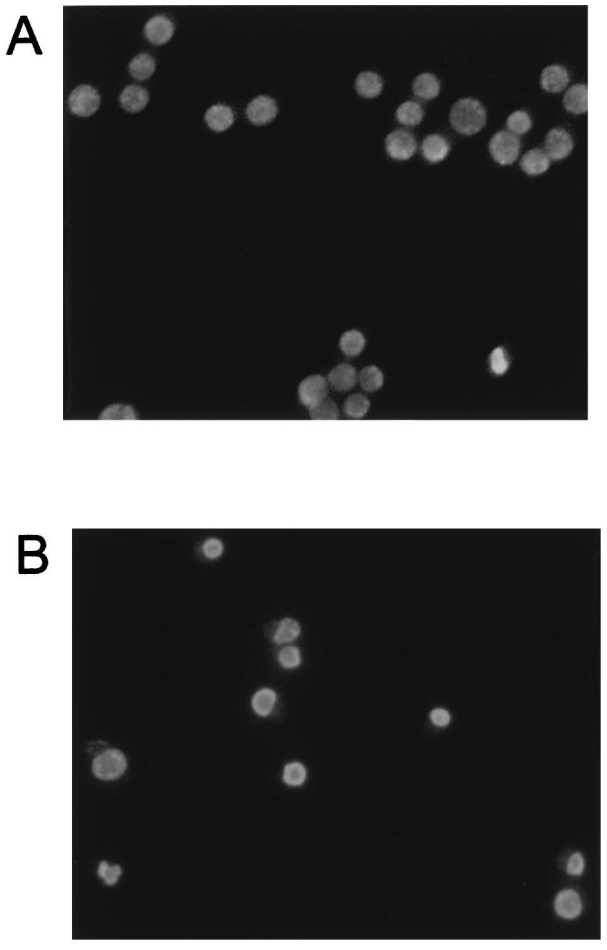

FIG. 6. Chromatin condensation in DBT cells infected with VV-E. DBT cells were mock infected (A) or infected with wt vaccinia virus (B) or VV-E (C) at an MOI of 1. At 42 h p.i., the cells were collected and stained with Hoechst 33342.

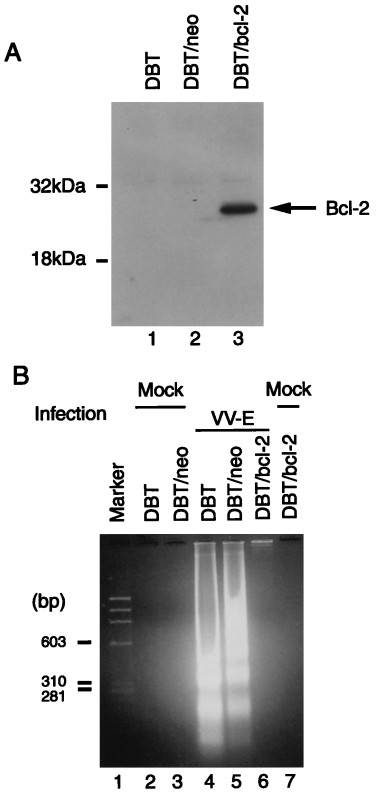

FIG. 7. Effect of high-level Bcl-2 expression on E protein-induced apoptosis. (A) Expression of Bcl-2 protein in DBT, DBT/neo, and DBT/bcl-2 cells. Proteins were separated, membranes were probed, and the signal was visualized as described in the text. (B) Inhibition of E protein-induced apoptosis in DBT/bcl-2 cells. DBT, DBT/neo, and DBT/bcl-2 cells were infected with VV-E at an MOI of 1 or mock infected, as indicated. At 48 h p.i., low-molecular-weight DNA was extracted and separated in a 2% agarose gel.

horseradish peroxidase. The signal was visualized by enhanced chemiluminescence (Amersham). We detected a high level of expression of Bcl-2 in DBT/bcl-2 cells but not in DBT and DBT/neo cells (Fig. 7A). DBT/bcl-2, DBT/neo, and DBT cells were infected with VV-E at an MOI of 1, and the low-molecular-weight DNA was extracted at 48 h p.i. Detection of internucleosomal DNA cleavage products by agarose gel electrophoresis showed that DNA fragmentation induced by VV-E infection was significantly inhibited in the DBT/bcl-2 cells but not in DBT/neo or DBT cells (Fig. 7B). Levels of expression of E protein in these cells were similar (data not shown). These data demonstrated that the apoptotic pathway induced by E protein was blocked by a high level of Bcl-2 expression, suggesting that the initiation of the apoptotic pathway activated by MHV E protein is likely located upstream of Bcl-2. In the study of TGEV-induced apoptosis, the authors discussed the inability of human Bcl-2 to block or delay apoptosis induced by TGEV infection (19).

We demonstrated induction of apoptosis in MHV-infected 17Cl-1 cells but not in MHV-infected DBT cells. It is not clear why apoptosis was not induced in MHV-infected DBT cells, since E protein expression driven by VV-E induced apoptosis in DBT cells. Production of MHV E protein must occur in MHV-infected DBT cells, because E protein is necessary for virus assembly (22). There are several possibilities to explain why apoptosis was not induced in MHV-infected DBT cells. One possibility is that the amount of E protein produced in MHV-infected DBT cells is too low to induce apoptosis. E protein synthesis was detectable by immunoprecipitation of [^{35}S]methionine-labeled proteins by using anti-E protein antibody in VV-E-infected DBT cells, whereas MHV-JHM E protein synthesis was difficult to demonstrate in MHV-JHM-infected DBT cells (data not shown). Probably the amount of E

protein in MHV-JHM-infected cells was too low to be detected. However, DBT cells infected with MHV-A59 synthesize approximately 10-fold-higher levels of E protein than MHV-JHM-infected DBT cells (data not shown), yet apoptosis was not induced in MHV-A59-infected DBT cells. Study of E protein-mediated apoptosis under an expression system, in which E protein expression level is regulated and vaccinia virus is not involved, will not only provide valuable information to address the question but also clarify whether some vaccinia virus function(s) might contribute to E protein-induced apoptosis. Another possibility is that apoptosis induction by the MHV E protein is somehow suppressed in MHV-infected DBT cells throughout infection. If this is the case, MHV infection in DBT cells may induce antiapoptosis function(s), which suppresses E protein-induced apoptosis.

Studies of porcine reproductive and respiratory syndrome virus (PRRSV), an arterivirus, demonstrated that PRRSV infection in established cell lines induces apoptosis (56). Arteriviruses are enveloped RNA viruses closely related to coronaviruses (6, 15). Expression of glycosylated membrane p25 protein of PRRSV by recombinant vaccinia virus also induces apoptosis, while overexpression of Bcl-2 does not prevent apoptosis induction by expressed PRRSV p25 (56). In contrast, overexpression of Bcl-2 inhibited MHV E protein-induced apoptosis. Although MHV E protein and PRRSV p25 are both viral structural envelope proteins, they are not homologs. In fact, the structural proteins of the arteriviruses and coronaviruses are unrelated, thus there is no arterivirus homolog to the E protein. The difference in the induction of apoptosis in the Bcl-2-overexpressing cells indicated that mechanisms of apoptosis induction by PRRSV p25 protein and MHV E protein are probably different.

The first two authors contributed equally to this study.

We thank Fumihiro Taguchi, National Institute of Neuroscience, Japan, for RVV t(+), Stephen A. Stohlman, University of Southern California, for vJN, vJM, and vJHE, J. Marie Hardwick, Johns Hopkins University, for plasmids pZIPneo and pZIPbcl-2, and Bernard Moss, NIH Laboratory of Viral Disease, for pSC11ss and pMJ601. We also thank John F. Repass and Sangeeta Banerjee for proofreading of the manuscript.

This work was supported by Public Health Service grant AI29984 from the National Institutes for Health (to S.M.) and grants from the National Multiple Sclerosis Society and the Stearman family (to J.L.L.).

REFERENCES

1. **Afonso, C. L., J. G. Neilan, G. F. Kutish, and D. L. Rock.** 1996. An African swine fever virus Bcl-2 homolog, 5-HL, suppresses apoptotic cell death. J. Virol. **70:**4858–4863.
2. **Bailey, O., A. M. Pappenheimer, F. S. Cheever, and J. B. Daniels.** 1949. A murine virus (JHM) causing disseminated encephalomyelitis with extensive destruction of myelin. II. Pathology J. Exp. Med. **90:**195–212.
3. **Baudoux, P., C. Carrat, L. Besnardeau, B. Charley, and H. Laude.** 1998. Coronavirus pseudoparticles formed with recombinant M and E proteins induce alpha interferon synthesis by leukocytes. J. Virol. **72:**8636–8643.
4. **Belyavskyi, M., E. Belyavskaya, G. A. Levy, and J. L. Leibowitz.** 1998. Coronavirus MHV-3-induced apoptosis in macrophages. Virology **250:**41–49.
5. **Bos, E. C. W., W. Luytjes, H. van der Meulen, H. K. Koerten, and W. J. M. Spaan.** 1996. The production of recombinant infectious DI-particles of a murine coronavirus in the absence of helper virus. Virology **218:**52–60.
6. **Cavanagh, D.** 1997. Nidovirales: a new order comprising Coronaviridae and Arteriviridae. Arch. Virol. **142:**629–633.
7. **Cepko, C. L., B. E. Roberts, and R. C. Mulligan.** 1984. Construction and applications of a highly transmissible murine retrovirus shuttle vector. Cell **37:**1053–1062.
8. **Chakrabarti, S., K. Brechling, and B. Moss.** 1985. Vaccinia virus expression vector: coexpression of β-galactosidase provides visual screening of recombinant virus plaques. Mol. Cell. Biol. **5:**3403–3409.
9. **Chiou, S. K., C. C. Tseng, L. Rao, and E. White.** 1994. Functional complementation of the adenovirus 19-kilodalton protein with Bcl-2 in the inhibition of apoptosis in infected cells. J. Virol. **68:**6553–6566.
10. **Chou, J., and B. Roizman.** 1992. The $\gamma_1$34.5 gene of herpes simplex virus 1 precludes neuroblastoma cells from triggering total shutoff of protein synthesis characteristic of programmed cell death in neuronal cells. Proc. Natl. Acad. Sci. USA **89:**3266–3270.
11. **Clem, R. J., M. Fechheimer, and L. K. Miller.** 1991. Prevention of apoptosis by a baculovirus gene during infection of insect cells. Science **254:**1388–1390.
12. **Cohen, G. M.** 1997. Caspases: the executioners of apoptosis. Biochem. J. **326:**1–16.
13. **Compton, S. R., S. W. Barthold, and A. L. Smith.** 1993. The cellular and molecular pathogenesis of coronaviruses. Lab. Anim. Sci. **43:**15–28. (Erratum, **43:**203.)
14. **Davison, A. J. and B. Moss.** 1990. New vaccinia virus recombination plasmids incorporating a synthetic late promoter for high level expression of foreign proteins. Nucleic Acids Res. **18:**4285–4286.
15. **de Vries, A. A. F., M. C. Horzinek, P. J. M. Rottier, and R. J. de Groot.** 1997. The genome organization of the Nidovirales: similarities and differences between arteri-, toro-, and coronaviruses. Semin. Virol. **8:**33–47.
16. **Dobbelstein, M., and T. Shenk.** 1996. Protection against apoptosis by the vaccinia virus SPI-2 (B13R) gene product. J. Virol. **70:**6479–6485.
17. **Dveksler, G. S., M. N. Pensiero, C. B. Cardellichio, R. K. Williams, G.-S. Jiang, K. V. Holmes, and C. W. Dieffenbach.** 1991. Cloning of the mouse hepatitis virus (MHV) receptor: expression in human and hamster cell lines confers susceptibility to MHV. J. Virol. **65:**6881–6891.
18. **Ekert, P. G., and D. L. Vaux.** 1997. Apoptosis and the immune system. Br. Med. Bull. **53:**591–603.
19. **Eleouet, J.-F., S. Chilmonczyk, L. Besnardeau, and H. Laude.** 1998. Transmissible gastroenteritis coronavirus induces programmed cell death in infected cells through a caspase-dependent pathway. J. Virol. **72:**4918–4924.
20. **Enari, M., H. Sakahira, H. Yokoyama, K. Okawa, A. Iwamatsu, and S. Nagata.** 1998. A caspase-activated DNase that degrades DNA during apoptosis, and its inhibitor ICAD. Nature **391:**43–50.
21. **Fernandez-Arias, A., S. Martinez, and J. F. Rodriguez.** 1997. The major antigenic protein of infectious bursal disease virus, VP2, is an apoptotic inducer. J. Virol. **71:**8014–8018.
22. **Fischer, F., C. F. Stegen, P. S. Masters, and W. A. Samsonoff.** 1998. Analysis of constructed E gene mutants of mouse hepatitis virus confirms a pivotal role for E protein in coronavirus assembly. J. Virol. **72:**7885–7894.
23. **Henderson, S., D. Huen, M. Rowe, C. Dawson, C. Dawson, G. Johnson, and A. Rickinson.** 1993. Epstein-Barr virus-coded BHFR1 protein, a viral homologue of Bcl-2, protects human B cells from programmed cell death. Proc. Natl. Acad. Sci. USA **90:**8479–8483.
24. **Henderson, S., M. Rowe, C. Gregory, C. D. Croom, F. Wang, R. Longnecker, E. Kieff, and A. Rickinson.** 1991. Induction of bcl-2 expression by Epstein-Barr virus latent membrane protein 1 protects infected B cells from programmed cell death. Cell **65:**1107–1115.
25. **Hinshaw, V. S., C. W. Olsen, N. Dybdahl-Sissoko, and D. Evans.** 1994. Apoptosis: a mechanism of cell killing by influenza A and B viruses. J. Virol. **68:**3667–3673.
26. **Hirano, N., K. Fujiwara, S. Hino, and M. Matsumoto.** 1974. Replication and plaque formation of mouse hepatitis virus (MHV-2) in mouse cell line DBT culture. Arch. Gesamte Virusforch. **44:**298–302.
27. **Houtman, J. J., and J. O. Fleming.** 1996. Pathogenesis of mouse hepatitis virus-induced demyelination. J. Neurovirol. **2:**361–376.
28. **Jacobson, M. D., M. Weil, and M. C. Raff.** 1997. Programmed cell death in animal development. Cell **88:**347–354.
29. **Jeurissen, S. H. M., F. Wangenaar, J. M. A. Pol, A. J. van der Eb, and M. H. M. Noteborn.** 1992. Chicken anemia virus causes apoptosis of thymocytes after in vivo infection and of cell lines after in vitro infection. J. Virol. **66:**7383–7388.
30. **Kim, K.-H., K. Narayanan, and S. Makino.** 1997. Assembled coronavirus from complementation of two defective interfering RNAs. J. Virol. **71:**3922–3931.
31. **Kozak, M.** 1986. Point mutations define a sequence flanking the AUG initiator codon that modulates translation by eukaryotic ribosomes. Cell **44:**283–292.
32. **Lai, M. M. C., and S. A. Stohlman.** 1978. RNA of mouse hepatitis virus. J. Virol. **26:**236–242.
33. **Lai, M. M. C., P. R. Brayton, R. C. Armen, C. D. Patton, C. Pugh, and S. A. Stohlman.** 1981. Mouse hepatitis virus A59: mRNA structure and genetic localization of the sequence divergence from hepatotropic strain MHV-3. J. Virol. **39:**823–834.
34. **Lane, T. E., and M. J. Buchmeier.** 1997. Murine coronavirus infection: a paradigm for virus-induced demyelinating disease. Trends Microbiol. **5:**9–14.
35. **Lee, H.-J., C.-K. Shieh, A. E. Gorbalenya, E. V. Koonin, N. La Monica, J. Tuler, A. Bagdzhadzhyan, and M. M. C. Lai.** 1991. The complete sequence (22 kilobases) of murine coronavirus gene 1 encoding the putative proteases and RNA polymerase. Virology **180:**567–582.
36. **Leibowitz, J. L., K. C. Wilhelmsen, and C. W. Bond.** 1981. The virus-specific intracellular RNA species of two murine coronavirus: MHV-A59 and MHV-JHM. Virology **114:**39–51.
37. **Levine, B., Q. Huang, J. T. Isaacs, J. C. Reed, D. E. Griffin, and J. M. Hardwick.** 1993. Conversion of lytic to persistent alphavirus infection by the

bcl-2 cellular oncogene. Nature **361:**739–742.
38. **Lowe, S. W., and H. E. Ruley.** 1993. Stabilization of the p53 tumor suppressor is induced by adenovirus 5 E1A and accompanies apoptosis. Genes Dev. **7:**535–545.
39. **Macen, J. L., K. A. Graham, S. F. Lee, M. Schreiber, L. K. Boshkov, and G. McFadden.** 1996. Expression of the myxoma virus tumor necrosis factor receptor homologue and M11L genes is required to prevent virus-induced apoptosis in infected rabbit T lymphocytes. Virology **218:**232–237.
40. **Mackett, M., G. L. Smith, and B. Moss.** 1984. General method for production and selection of infectious vaccinia virus recombinants expressing foreign genes. J. Virol. **49:**857–864.
41. **McCarthy, S. A., H. S. Symonds, and T. Van Dyke.** 1994. Regulation of apoptosis in transgenic mice by simian virus 40 T antigen-mediated inactivation of p53. Proc. Natl. Acad. Sci. USA **91:**3979–3983.
42. **Meyaard, L., S. A. Otto, R. R. Jonker, M. J. Mijnster, R. P. M. Keet, and F. Miedema.** 1992. Programmed death of T cells in HIV-1 infection. Science **257:**217–219.
43. **Milligan, C. E., and L. M. Schwartz.** 1997. Programmed cell death during animal development. Br. Med. Bull. **52:**570–590.
44. **Morey, A. L., D. J. Ferguson, and K. A. Fleming.** 1993. Ultrastructural features of fetal erythroid precursors infected with parvovirus B19 in vitro: evidence of cell death by apoptosis. J. Pathol. **169:**213–220.
45. **Nicholson, D. W., and N. A. Thornberry.** 1997. Caspases: killer proteases. Trends Biochem. Sci. **22:**299–306.
46. **Pachuk, C. J., P. J. Bredenbeek, P. W. Zoltick, W. J. M. Spaan, and S. R. Weiss.** 1989. Molecular cloning of the gene encoding the putative polymerase of mouse hepatitis virus, strain A59. Virology **171:**141–148.
47. **Pugachev, K. V., and T. K. Frey.** 1998. Rubella virus induces apoptosis in culture cells. Virology **250:**359–370.
48. **Rao, L. M., M. Debbas, P. Sabbatini, D. Hockenberry, S. Korsmeyer, and E. White.** 1992. The adenovirus E1A proteins induce apoptosis, which is inhibited by the E1B 19Ka and Bcl-2 proteins. Proc. Natl. Acad. Sci. USA **89:** 7742–7746.
49. **Rowe, C. L., S. C. Baker, M. J. Nathan, and J. O. Fleming.** 1997. Evolution of mouse hepatitis virus: detection and characterization of spike deletion variants during persistent infection. J. Virol. **71:**2959–2969.
50. **Shibata, S., S. Kyuwa, S.-K. Lee, Y. Toyoda, and N. Goto.** 1994. Apoptosis induced in mouse hepatitis virus-infected cells by a virus-specific $CD8^+$ cytotoxic T-lymphocyte clone. J. Virol. **68:**7540–7545.
51. **Smyth, M. J., and J. A. Trapani.** 1998. The relative role of lymphocyte granule exocytosis versus death receptor-mediated cytotoxicity in viral pathophysiology. J. Virol. **72:**1–9.
52. **Stohlman, S. A., S. Kyuwa, J. M. Polo, D. Brady, M. M. C. Lai, and C. C. Bergmann.** 1993. Characterization of mouse hepatitis virus-specific cytotoxic T cells derived from the central nervous system of mice infected with the JHM strain. J. Virol. **67:**7050–7059.
53. **Stohlman, S. A., S. Kyuwa, M. Cohen, C. Bergmann, J. M. Polo, J. Yeh, R. Anthony, and J. G. Keck.** 1992. Mouse hepatitis virus nucleocapsid protein-specific cytotoxic T lymphocytes are L^d restricted and specific for the carboxy terminus. Virology **189:**217–224.
54. **Sturman, L. S., and K. K. Takemoto.** 1972. Enhanced growth of a murine coronavirus in transformed mouse cells. Infect. Immun. **6:**501–507.
55. **Sturman, L. S., K. V. Holmes, and J. Behnke.** 1980. Isolation of coronavirus envelope glycoproteins and interaction with the viral nucleocapsid. J. Virol. **33:**449–462.
56. **Suarez, P., M. Diaz-Guerra, C. Prieto, M. Esteban, J. M. Castro, A. Nieto, and J. Ortin.** 1996. Open reading frame 5 of porcine reproductive and respiratory syndrome virus as a cause of virus-induced apoptosis. J. Virol. **70:**2876–2882.
57. **Taguchi, F., T. Ikeda, and H. Shida.** 1992. Molecular cloning and expression of a spike protein of neurovirulent murine coronavirus JHMV variant cl-2. J. Gen. Virol. **73:**1065–1072.
58. **Tewari, M., and V. M. Dixit.** 1995. Fas- and tumor necrosis factor-induced apoptosis is inhibited by the poxvirus crmA gene product. J. Biol. Chem. **270:**3255–3260.
59. **Thoulouze, M.-I., M. Lafage, J. A. Montano-Hirose, and M. Lafon.** 1997. Rabies virus infects mouse and human lymphocytes and induces apoptosis. J. Virol. **71:**7372–7380.
60. **Vennema, H., G.-J. Godeke, J. W. A. Rossen, W. F. Voorhout, M. C. Horzinek, D.-J. E. Opstelten, and P. J. M. Rottier.** 1996. Nucleocapsid-independent assembly of coronavirus-like particles by co-expression of viral envelope protein genes. EMBO J. **15:**2020–2028.
61. **Wege, H., S. Siddell, and V. ter Meulan.** 1982. The biology and pathogenesis of coronaviruses. Curr. Top. Microbiol. Immunol. **99:**165–200.
62. **Welsh, R. M., M. Y. Lin, B. L. Lohman, S. M. Varga, C. C. Zarozinski, L. K. Selin.** 1997. Alpha beta and gamma delta T-cell networks and their roles in natural resistance to viral infections. Immunol. Rev. **159:**79–93.
63. **Yokomori, K., M. Asanaka, S. A. Stohlman, S. Makino, R. A. Shubin, W. Gilmore, L. P. Weiner, F.-I. Wang, and M. M. C. Lai.** 1995. Neuropathogenicity of mouse hepatitis virus JHM isolates differing in hemagglutinin-esterase protein expression. J. Neurovirol. **1:**330–339.
64. **Yu, X., W. Bi, S. R. Weiss, and J. L. Leibowitz.** 1994. Mouse hepatitis virus gene 5b protein is a new virion envelope protein. Virology **202:**1018–1023.
65. **Zhu, H., Y. Shen, and T. Shenk.** 1995. Human cytomegalovirus IE1 and IE2 proteins block apoptosis. J. Virol. **69:**7960–7970.